西安交通大学
XI'AN JIAOTONG UNIVERSITY

World Scientific
www.worldscientific.com

Effect of doping in multiferroic BFO: A review

A. Joana Preethi and M. Ragam[*]

Research Centre of Physics, Fatima College (Autonomous)

Madurai 625018, Tamil Nadu, India

[*]*mraagam.physics@gmail.com*

Bismuth ferrite (BFO) nanostructures and thin films have gained attraction as suitable candidates for energy storage and energy conversion due to their high energy storage efficiency, temperature stability and low dielectric loss. Electrical properties of such multiferroic materials are tailored by ferroelectric and ferromagnetic constituents and have opened up amazing avenues in electrochemical supercapacitor and photovoltaic applications. Dopants play a significant role in optimizing the magnetic and dielectric properties of such materials owing to suitable applications. This review highlights the scientific advancements reported in BFO nanostructures for energy applications by optimizing their magnetic and dielectric properties. This paper starts with a brief introduction of BFO and a discussion on the effects of various dopants by different synthesis techniques, and their effects on the magnetic and dielectric properties are also portrayed. Eventually, this review summarizes the various doping effects, which paves way for future research on this multiferroic material.

Keywords: BFO; multiferroic; ferromagnetic; ferroelectric; dielectric property; magnetoelectric coupling.

Highlights

- The preparation of various multiferroic BFO-based nano-materials and nanocomposites is summarized.
- *A*-site substitution improves the magnetization and dielectric properties.
- *B*-site doping reported enhanced magnetic properties making them suitable candidates for supercapacitor applications.
- BFO thin films showed enhanced dielectric properties due to their thickness and their epitaxial strain.
- BFO composites were reviewed and reported to offer higher magnetoelectric effect.

1. Introduction

The production of energy is currently moving towards more eco-friendly solutions such as wind turbines, solar panels and geothermal plants; however, the storage of this energy still mostly relies on batteries. Modern batteries often use environmentally unfriendly materials (lithium, lead–acid, etc.) and have relatively short life cycle. Supercapacitors, i.e., ultracapacitors/electrochemical double-layer supercapacitors, offer potential alternatives to batteries, as they present an opportunity to utilize greener materials, have longer lifetime (withstanding a half-million cycles or more), high charge and discharge rates and high power density.

Recently, dielectric materials with high energy storage density, good temperature stability and low dielectric loss have gained potential applications in capacitor technology. Developing capacitors with improved energy density, storage efficiency and operation sustainability in severe environments is one of the main aims of the ceramic industries.[1] The electrochemical batteries possess high energy density and low power density,[2] while capacitors have high power density and low energy density. To enhance the features of present electrochemical energy storage devices, the dielectric properties of capacitors need to be optimized and finding a suitable dielectric material is vital for industrial applications.[2]

Materials that possess high electrical resistivity are called dielectrics and can exhibit paraelectric, ferroelectric (FE) and piezoelectric behaviors. In the case of paraelectric and ferroelectric behaviors, an applied electric field induces a change in polarization, while for piezoelectrics, the effect is due to the application of pressure or temperature, respectively.[3] Capacitor dielectrics and piezoelectric devices are among the many other application areas of ceramics. If they persist for a long operation time in extreme physical conditions such as temperature or pressure, ceramics are considered the prime choice for use when compared to metals and plastics. Dielectric properties such as relative permittivity and dielectric loss factor of ceramic material are affected significantly as frequency changes, therefore their ranges have to be determined before the design of any system containing their utilization. Thus, research in ceramic technology is currently flourishing with rapid demand to obtain materials with the required properties.[4]

*Corresponding author.

In this review, we will specifically focus on bismuth ferrite (BFO or BiFeO$_3$) material, its dielectric and energy storage properties and its applications. Multiferroics exhibit simultaneous polar and magnetic orders, as in the cases of strong magnetoelectric (ME) coupling both the magnetization and polarization can be manipulated by electric as well as magnetic fields. Among all the multiferroic materials of type ABO_3, BFO is the most promising single-phase multiferroic material exhibiting multiferrocity at room temperature.[5] It has a distorted rhombohedral perovskite (ABO_3) structure with $R3c$ space group which is noncentrosymmetric. The magnetoelectric effect in a material can be defined as the electric polarization induced by applied magnetic field or vice versa (the magnetization induced by applied electric field). Both ferroelectricity and antiferromagnetism are reported in BiFeO$_3$ single crystals.[6] It is an eco-friendly material free of lead and has interesting multiferroic as well as optical properties. However, its secondary phases during the synthesis, weak magnetic characteristics, low magnetoelectric coupling and high leakage current[7,8] make it of limited applicability. The limitations of BFO can be overcome by cautious synthesis, doping and coating with other materials. It was noted that the physical properties of BiFeO$_3$ can be enhanced through doping by increasing the oxygen vacancy, strain state and bandgap. Moreover, the rare-earth metal doping can improve the high leakage current density and weak ferromagnetism. Under this condition, several studies relating to functional properties improvement of BiFeO$_3$ through doping at both the Bi and Fe sites have been made and reported successfully the substitution of rare-earth ions (La, Pr, Gd, Ho, Eu, Nd, etc.) at the Bi site[9–14] or doping of transition metal ions (Ti, Cr, Co, Mn, etc.)[15–18] at the Fe site.

This review paper aims to offer a systematic review of dielectric properties of pure and doped BFO-based nanostructures.

2. Dielectric Properties for Energy Storage

Dielectrics are grouped according to the relation between the applied field and the polarization. For linear dielectrics, the energy density (u) is expressed as: $u = 1/2\varepsilon_0\varepsilon_r E^2$. For nonlinear dielectrics, the polarization can be determined from the polarization–electric field (P–E) hysteresis measurements by: $P = \varepsilon_0(\varepsilon_r - 1)E = \chi_e\varepsilon_0 E$, where P is polarization and χ_e is dielectric susceptibility. Energy density (u) is said to be a measure of energy stored per unit volume. For dielectrics, the energy storage density can be obtained by: $u = \int_0^{E\max} PdE$.

Using the above equation, the energy density values of dielectrics can be obtained by using the numerical integration of area between the curves of polarization and electrical field (i.e., P–E loops). It can be concluded from the above equations that larger energy densities can be obtained by greater relative permittivity, highest polarization and breakdown strength, while low dielectric losses, reduced remnant polarizations and smaller value of loss tangent (tan δ) will ensure greater energy storage efficiencies of dielectric materials. In this review, we describe the reported works to optimize these properties under different conditions to reduce the limitations of BFO in industry.

3. Dielectric Materials for High Energy Storage Applications

To design a good dielectric material with high energy storage density and higher efficiency for the required application, high breakdown strength,[19] large saturated polarization and small remanent polarization[20] should be satisfied simultaneously.[21] Among the four main categories of dielectric materials which are the linear dielectric, ferroelectric, relaxor ferroelectric (RFE) and antiferroelectric materials, only two of them, namely the relaxor ferroelectrics and antiferroelectrics, are more suitable for high energy storage applications due to their high saturated polarization and low remnant polarization. Each of them is described by the P–E loop given in Fig. 1(b). Furthermore, the RFE dielectrics can be further classified into lead-based and lead-free RFE dielectrics. The following subsections describe the dielectric properties of both of them to analyze their multifunctional properties.

3.1. *Dielectric properties of pure BFO nanostructures*

BFO is one of the rare multiferroic compounds in which ferroelectricity and magnetism coexist at room temperature. It has been synthesized in bulk form, thin-film form and as nanostructures. This material has gained considerable attention because of its fundamental coupling phenomena of multiple-order parameters and practical applications in magnetoelectric devices based on electrically controlled magnetism.[23–25] Bulk BFO has rhombohedral symmetry ($R3c$ space group) with ferroelectric polarization.[26–29] The polarization is mainly caused by Bi^{3+} lone pair (6s^2 orbital), i.e., the polarization originates mostly from A-site while the magnetization comes from Fe^{3+}, i.e., the B-site.

Perovskite (ABO_3) BFO has Fe^{3+} ions at B-sites surrounded by six neighboring oxygen anions forming the FeO$_6$ octahedral. Empty spaces, i.e., A-sites, between the FeO$_6$ backbones are occupied by Bi^{3+} ions. Such perovskite structures are formed by occupying B-sites usually with transition metal ions and by filling A-sites with trivalent rare-earth ions or divalent rare-earth ions. It is believed that the physical properties of perovskite compounds are mainly due to transition metal ions located at B-sites and electronic conduction is affected by the chemical bonding between Fe^{3+} and O ions.

The effects of annealing temperature on the structure, morphology, dielectric and magnetic properties of sol–gel-synthesized multiferroic BiFeO$_3$ nanostructures were reported in recent studies that provide a base for reliable research on the ferroelectric and magnetoelectric properties. Ranjbar *et al*.[30] have reported pure BFO phase at an annealing temperature of 800°C. An appreciable magnetic behavior was noted
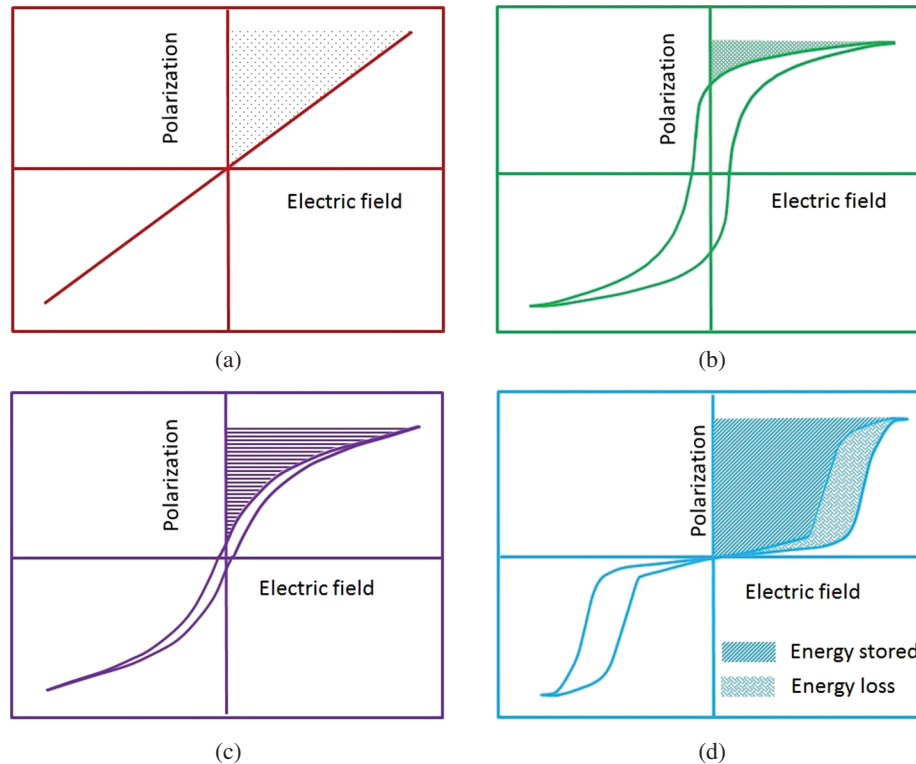
Fig. 1.   The typical polarization versus electric field hysteresis loops and the energy storage characteristics of the four classes of solid dielectric materials, namely (a) linear, (b) ferroelectric, (c) relaxor ferroelectric and (d) antiferroelectric materials.[22]

Note: Demonstration only; not to scale.

by the vibrating sample magnetometer at 800°C due to its response with respect to its periodic spin structure and wavelength. Further, a decrease in the relative dielectric constant was reported as a sign of decreasing oxygen valences at high temperature. The hysteresis curves for samples were reported by vibrating sample method at room temperature. Saturation magnetization of the sample annealed at 700°C was reported as the highest than others which could be due to the presence of $Bi_{25}FeO_{40}$ magnetic impurity phases.[30]

Kumari *et al.*[6] have investigated and reported the details of microstructural, magnetic, electrical and magnetocapacitance (MC) properties of pure BFO nanoparticles (average particle size ~80 nm) synthesized by novel chemical citrate sol–gel route. Appreciable change of dielectric constant with the magnetic field was reported which revealed the presence of magnetoelectric coupling in nanoparticles. The observed ferromagnetic (FM) *M–H* loop, ferroelectric *P–E* loop and significant magnetocapacitance at room temperature in the nanometric form make the material useful in comparison with its bulk counterpart for technologically potential device applications.[6]

The structural, thermal, microscopic, magnetization, polarization and dielectric properties of $BiFeO_3$ ceramics synthesized by a rapid liquid-phase sintering technique were reported by Pradhan *et al.*[31] The magnetization and ferroelectric properties were reported to be enhanced. The reduced

polarization was due to the high loss and low dielectric permittivity of the ceramic, reported to be caused by higher leakage current. The numerical values of the reported results of spontaneous polarization, remnant polarization and coercive fields are about 3.5 μC/cm^2, 2.5 μC/cm^2 and 40 kV/cm, respectively.

Single-crystal-like $BiFeO_3$ thin films were fabricated by flux-mediated epitaxy (FME) using pulsed laser deposition (PLD) by Lim *et al.*,[32] and various properties were reported. The growth conditions were optimized and the size of the single crystal was found to be increased for the FME grown crystals. A higher dielectric constant was reported in the range of 260–340 than those for the standard PLD grown films. In addition, the leakage current density of the films was reduced by two orders of magnitude compared to that of standard PLD grown films.[32]

$BiFeO_3$ powders were derived by molten salt method in NaCl media by Zheng *et al.*[33] The average grain size of power was reported to decrease with the increase of NaCl content. Higher dielectric constant and lower dielectric loss were reported in the $BiFeO_3$ ceramics derived from a higher salt ratio.[33] Table 1 provides a summary of the $BiFeO_3$ nanomaterials synthesized. $BiFeO_3$ nanomaterials have been synthesized so far using several techniques, including sol–gel, sonochemical, reverse micelle, coprecipitation, combustion, etc.

Table 1.   Summary of BiFeO$_3$ nanostructures.[34]

Morphology	Fabrication method(s)	Source
Nanopowders	Solution combustion, sol–gel methods	Refs. 35 and 36
Microrods	Polymer-directed solvothermal method	Ref. 37
Nanotubes	Template-induced sol–gel method	Refs. 38 and 39
Nanoflakes	Hydrothermal (HT) method	Ref. 40
Nanorods	Sonochemical method	Ref. 41
Submicron	Spindles hydrothermal method	Ref. 42
Nanowires	Anodized alumina template method	Ref. 43
Nanofibers	Sol–gel-based electrospinning method	Ref. 44
Nanocubes	Microwave synthesis method	Ref. 45

With the advancement in synthesis techniques for the fabrication of high-quality ceramics, multiferroic materials have attracted a great deal of technological and economic attention, especially to materials with an ABO_3 perovskite structure.[46,47] Currently, various methods have been developed for the preparation of micrometer- and nanometer-sized BFO crystallites. As we know, the classical HT synthesis is often used due to its simple control of grain size and morphology.[48] The improved dielectric properties of the prepared BFO nanostructures depend on the shape and size of the synthesized materials.

Many works were reported on the clarification of the structural and magnetic properties of BFO; a revival has been triggered by the general focus on multiferroics in the materials-based community and by the observation of weak ferromagnetism coexisting with ferroelectricity.[29] However, pure BFO suffers from impurity phases, magnetic defects from the ideal oxygen stoichiometry mimicking weak ferromagnetism and a number of further magnetic or structural phase transitions at low temperature.

4.   Doped BFO Nanostructures

4.1   *A-site doping*

A-site substitution refers to the case where the Bi^{3+} ions are replaced by the other ions. Since the electric levels of *A*-site ions are located far away from the Fermi level, the *A*-site substitution can influence the band structure indirectly.[49] *A*-site substitutions by some ions with smaller ionic radius can reduce the Fe–O–Fe bond angle accompanying a smaller tolerance factor leading to more insulating characters.

High level of doping goes beyond simply modifying the properties and leads to additional properties relating to the presence of oxygen vacancies. Here, we briefly review the recent findings focused on *A*-site-substituted BFO.

There exists a close link between crystallographic structure, polarization orientation and its electrochemical response. Also, the ferroelectric, dielectric and piezoelectric properties are strongly dependent on the ionic size of the substitution elements.

4.1.1.   *Ba-doped BFO nanostructures*

In 2019, Wu and Zhu[50] studied and reported on the $Bi_{1-x}Ba_x$-FeO_3 ($x = 0$–0.20) nanoparticles which were synthesized by molten solid-state method. XRD patterns demonstrated that all the $Bi_{1-x}Ba_xFeO_3$ nanoparticles crystallized in the rhombohedral structure with a space group of $R3c$. The SEM images demonstrated that the particle sizes decreased with increasing the Ba doping content, and the morphology of the particles changed from cubic or rectangular to spherical shape. An enhancement of the magnetization of the Ba-doped BFO (BBFO) nanoparticles was reported, which was due to the broken balance of the original spiral spin structure. Moreover, with the increase of the Ba doping content, the leakage current densities of the nanoparticles were decreased by one order of magnitude due to the suppression of impurity phases and oxygen vacancies, and the enhancement in dielectric properties was also reported.[50] The remanent magnetization of the BBFO nanoparticles was 0.51 emu/g. The leakage current density of the BBFO nanoparticles was measured to be only 1.15 nA/cm^2 whereas for the undoped BFO nanoparticles, it was 10.1 nA/cm^2. In addition to that, the dielectric properties of nanoparticles are also affected by the particle size. Here, the smaller grain sizes of the Ba-doped BFO nanoparticles lead to the lower dielectric constants due to the particle size effects.[51] The ferroelectric properties like enhanced remnant polarization (P_r) and lower leakage current density were reported due to the structural distortion. The reduction of dielectric loss with increasing the Ba doping content could be ascribed to the depression of the oxygen vacancies by Ba doping.[51] The remnant polarization value tends to increase and then decreases due to the charge fluctuation between Fe^{3+} and Fe^{2+} ions.

The physical and chemical properties of any material can be categorized into intrinsic and extrinsic properties. The dielectric properties of ferroelectric ceramics are generally influenced by their intrinsic and extrinsic contributions. In ferroelectric ceramics, the intrinsic contribution is generally the lattice distortion (change in size, shape and orientation) and the extrinsic contribution is mainly derived from domain wall motion.[155,156] Here, in the above context, the changes in the electrical properties were reported due to the change in their structure which is an intrinsic property.

The enhancement of magnetization and the decrease of leakage current density as well as the improved dielectric properties of the Ba-doped BFO nanoparticles have made them a promising candidate for applications not only in the field of nanospintronics but also in dielectric energy storages.

Das and Mandal[52] reported that the magnetic and ferroelectric properties of BFO are found to change significantly with Ba substitution in place of Bi. Canting of spins and displacement of oxygen atoms from their original position were reported to be the reasons for enhanced magnetic and ferroelectric properties, respectively. A noticeable change in dielectric constant with doping was observed. Magnetoelectric coupling also increased due to Ba substitution. A remarkable difference in dielectric constant above the magnetic transition temperature of the parent compound was reported using the electrical property measurements. Impact of dielectric properties is reflected in the reported remnant polarization (14.35 μC/cm^2) throughout the measurement cycles. It was also reported that the enhancement of the ferroelectric polarization was due to the reduced leakage current in the doped sample.

In multiferroics where the electric and magnetic domains coexist, the application of magnetic field gives rise to strain and hence a stress is developed. Strain-induced stress on the ferroelectric generates the electric field which could orient the ferroelectric domains, leading to modification of the dielectric properties.[52]

Hasan *et al*.[53] in 2016 derived Ba-doped BFO nanoparticles using sol–gel technique. The coercivity of the synthesized nanoparticles was also found to decrease significantly with reducing the particle size and becomes almost negligible. This indicates their soft nature which makes them potential candidates in device applications where a negligible coercivity at room temperature is crucially effective. Particle size-dependent polarization was reported in Ba-doped BFO[53] which is an intrinsic contribution. Thus, tuning of multiferroic properties by controlling the particle size paves way for its application in miniature devices.

Yang *et al*.[54] prepared Ba-doped BFO nanocrystals using sol–gel method and the properties were studied and reported. It was observed that with the transformation of crystal structure, the dispersion of the dielectric constant and loss of samples were changed. The increase in dielectric constant and decrease in dielectric loss were explained by the interfacial polarization in which the space charges tend to accumulate around the interfaces between the face of the samples and the electrode under an applied electric field and form an interfacial layer with a high relative dielectric constant and a low dielectric loss.[54] Magnetic properties were also greatly improved due to the presence of oxygen deficiency. They concluded that the BBFO$_x$ (Ba-doped BFO) nanocrystallite is promising for applications in data storage media.

The effects of oxygen annealing on the magnetic, electrical and magnetodielectric properties of Ba-doped BiFeO$_3$ particles prepared by the solid-state reaction method were investigated and reported Singh an Jung[55] in 2010. The magnetic properties were reported to be drastically changed from weak ferromagnetism to antiferromagnetism for oxygen-annealed BBFO at 850°C. The activation energies of as-grown BBFO and annealed BBFO were reported to be 0.40 eV and 0.73 eV,

respectively.[55] Magnetodielectric coupling was found to be larger for as-grown BBFO than for annealed BBFO, probably due to the ferromagnetic and antiferromagnetic (AFM) natures of the former and the latter.

Hence, Ba doping significantly influenced the structural, magnetic and dielectric properties of BiFeO$_3$. An increase in magnetic property was reported with increasing Ba doping.[56] The dielectric property was enhanced with increasing temperature because of the contribution of the space-charge polarization due to the presence of oxygen ion vacancies. The addition of Ba was reported to reduce the leakage current by filling the vacant Bi^{3+} sites and by decreasing the transition of Fe^{3+} ions to Fe^{2+} ions.[56]

4.1.2. *Pb-doped BFO nanostructures*

Lead is one of the most significant materials that are used in energy storage applications. The main reason for using lead in batteries is that it can store a lot of charge and provide high current for short periods of time. Hence, the lead atoms play a vital role in increasing the efficiency of supercapacitors.

Pb-doped BiFeO$_3$ (Bi$_{1-x}$Pb$_x$FeO$_3$, x=0.03–0.07) powders were reported by Mazumder and Sen.[57] The dielectric constant and the dissipation factor were reported to decrease with increasing frequency. The lower dielectric constant of lead-doped BiFeO$_3$ compared to pure BiFeO$_3$ was attributed to higher space-charge polarization in Pb-doped samples. The Pb addition increased the electrical resistivity and with increased lead doping, BiFeO$_3$ ceramics showed typical non-lossy ferroelectric hysteresis loops.

The effect of Pb-doped La$_{0.1}$Bi$_{0.9-x}$Pb$_x$FeO$_3$ samples, prepared by sol–gel auto-ignition technique, had been investigated and reported systematically.[58] An increase in grain size and porosity of the samples was found to be evident with Pb doping. The La doping changes the structure of BFO from rhombohedral to pseudotetragonal,[62] whereas Pb doping changes its structure to pseudocubic.[61,62] The value of the dielectric constant was found to be decreased with Pb doping. This anomalous behavior was reported due to the combined response of dielectric relaxation that involves the oriental polarization and the conduction of charge carriers.[63] It was reported that the dielectric loss also follows the same trend as dielectric constant. Similar trend of dielectric properties has also been reported in Mn-doped,[64] Sr-doped,[65] Sm-doped,[59] Pr-doped[60] and Dy-doped[66] BFO materials. A slight increase in these dielectric parameters was evident with the rise of temperature which can be attributed to the thermally induced enhancement of hopping conduction mechanism.[57,67] The structural transformation from rhombohedral to pseudocubic is almost complete and destroys the spatial spin structure[61] resulting in large latent magnetization as compared to other samples.[58]

Sr and Pb codoped BiFeO$_3$ compounds were reported by the rapid solid-state reaction method.[68] The results of XRD and Raman spectra revealed a transformation of the crystal

structure from rhombohedral to cubic with Sr/Pb doping. It was found that both ε_r and tan δ decrease with increasing frequency in the lower-frequency range, and almost become a constant in the higher-frequency range. The variations of ε_r at low frequency were explained by Maxwell–Wagner model involving space-charge polarization.[69] The reduction of leakage current is due to the reduction in oxygen vacancies. It was reported that the enhancement in ferromagnetic property is attributed to the collapse of the spiral cycloid and the release of latent magnetization due to the structural transition.[70]

Ca and Pb codoped polycrystalline BFO ceramics were successfully synthesized by the rapid solid-state reaction.[71] Investigations by XRD and Raman spectra reveal a crystal structural transition from rhombohedral to cubic with increasing Ca/Pb content.

The increase in dielectric constant due to increase in doping concentration was attributed to reduction of defects during heat treatment.[70] The reduction in dielectric loss factor with increasing the doping content suggests that the increase in Ca/Pb doping is helpful in reducing the leakage current. Ferroelectric remnant polarization and leakage current of Ca/Pb codoped BFO were reported to be improved significantly when compared to the undoped samples.[71]

4.1.3. *Rare-earth material-doped BFO nanostructures*

The unique magnetic, electrical and spectroscopic properties of rare-earth elements improve the efficiencies of energy conversion processes.[72] Pure and Sm-doped BFO particles were synthesized using sol–gel method by Rhaman *et al.*[73] in 2019. The substitution of Sm in BFO resulted in the structural transformation from rhombohedral to orthorhombic symmetry with decreased crystallite size. With increasing Sm dopant concentration, an increase in dielectric constant was reported which decreased with increasing frequency. The increase in dopant concentration resulted in a decrease in dielectric loss which was due to structural stability and less impurity phases. On increasing the dopant concentration, the maximum polarization was reported to be increased which caused the reduction in leakage current density due to the suppression of impurity phases.[73]

The electrical resistance, reactance and resistivity of doped samples were reported to be decreased considerably at low frequency and almost constant at high frequency.

Thus, the enhanced properties indicate that the Sm-doped BFO may be a potential candidate for memory devices, PV solar cells and energy storage devices. Table 2 summarizes the reported results of various Sm-doped BFO nanostructures.

La-doped $BiFeO_3$ (BLFO) nanoparticles have been successfully synthesized using nonvacuum sol–gel technique in 2016 by Awan *et al.*[78] The La-doped $BiFeO_3$ nanoparticles prepared using a dopant concentration of 0.3 wt% reported strong ferromagnetic behavior. It was reported that ferromagnetism in $BiFeO_3$ arises due to linearity in spin structure.

Anomalous dispersion was reported for the dielectric constant, while normal dispersion behavior was observed for tangent loss data. Dielectric constant increased and tangent loss decreased with the increase in dopant concentration. Table 3 summarizes the results of various La-doped BFO nanostructures synthesized by various methods.

The $Bi_{1-x}Y_xFeO_3$ (x=0, 0.1, 0.15, 0.2) nanoparticles were developed via sol–gel auto-combustion route by Sheoran *et al.*[84] It was reported that as the doping concentration increased, the grain size decreased. The reported value of remnant polarization (P_r) was increased with increasing the concentration of yttrium. Further, the structural transformation also is an important factor for the enhancement in polarization. With increasing Y concentration, the optical bandgap was reported to decrease which was similar to the earlier reported result by Fki *et al.*[85] This reduction in the bandgap of all Y^{3+}-substituted BFO samples can be caused by the enhancement in the internal chemical pressure and reduced oxygen vacancies located at FeO_6.[86] Also, the observed values of bandgap are lower than the earlier reported results of Y-substituted BFO nanoparticles.[85,87]

The dielectric constant value was reported to increase with increasing doping concentration. Temperature-dependent dielectric constant and loss reveal an abnormality in the temperature range of 370–410°C as a consequence of indirect magnetoelectric coupling.[84] The significant properties

Table 2.   Summary of reported Sm-doped BFO nanostructures.

Method of synthesis	Structure	Reported significance	Source
Tartaric acid-assisted sol–gel technique	Orthorhombic	Magnetic properties were enhanced	Ref. 74
Modified solid-state reaction method	Tetragonal	The pyroelectric and piezoelectric coefficients increased with increase in doping concentration	Ref. 75
Conventional solid-state method	Rhombohedral	Dielectric permittivity and dielectric loss were decreased with increasing frequency. Lower dielectric property on doping implied enhanced magnetic and ferroelectric properties	Ref. 76
Modified rapid liquid-phase sintering method	Rhombohedral	Enhanced magnetization and thermal stability with increasing doping concentration	Ref. 77

Table 3.   Summary of reported La-doped BFO nanostructures.

Method of synthesis	Structure(s)	Reported significance	Source
Sol–gel method	Rhombohedral	Decrease in bandgap and remnant polarization with increasing La concentration	Ref. 79
Pechini method	Rhombohedral	Enhancement in the permittivity, ferroelectric and ferromagnetic properties and less electrical leakage	Ref. 80
Hydrothermal method	Rhombohedral, cylindrical-shaped	Enhancement of magnetization due to the breaking of the spin cycloid and increase in dielectric constant	Ref. 81
Hydrothermal technique	Rhombohedral	Dielectric constant was enhanced fourfold after La doping at room temperature. Magnetic moment increased up to 0.658 emu/g on doping	Ref. 82
Solid-state reaction route	Hexagonal	Increases in the magnetic anisotropy and magnetization and observation of exchange bias	Ref. 83

Table 4.   Summary of reported Y-doped BFO nanostructures.

Method of synthesis	Structure(s)	Reported significance	Source
Sol–gel-based electrospinning process	Orthorhombic, nanofiber	Lower dielectric loss and more dependence of capacitance on bias voltage and decreased leakage current on doping	Ref. 88
Solid-state reaction technique	Orthorhombic, cubic	Improved magnetic and dielectric behaviors	Ref. 89
Metal ion ligand complex-based precursor-solution evaporation method	Varies from rhombohedral to tetragonal as the doping concentration increases	Enhanced magnetic, ferroelectric properties and improved magnetoelectric coupling	Ref. 90
Auto-combustion method	Orthorhombic	Improved electrical and magnetic properties	Ref. 91

reported via different synthesis procedures are tabulated in Table 4.

Pure and Gd-doped bismuth ferrite samples were successfully synthesized using sol–gel method by Vashisth *et al*. in 2018.[92] XRD analysis revealed that all of these samples existed in rhombohedral structure. There is an enhancement in ferromagnetic nature such as the increments in the observed saturation polarization (P_s), remanent polarization (P_r) and coercive field (E_c), and their numerical values are reported to be 0.334 $\mu C/cm^2$, 0.041 $\mu C/cm^2$ and 3.850 kV/cm for all Gd-doped samples as compared to the undoped BFO. The dielectric behavior depends on the space-charge contributions to polarization.[92] The dielectric constant of samples increased with doping. Gd-doped BFO nanostructures prepared by various methods are summarized in Table 5.

Cyriac *et al*. in 2019[98] successfully prepared the single-phase nanocrystalline multiferroic $Bi_{1-x}Eu_xFeO_3$ ($x = 0$–0.3) materials by sol–gel method. The substitution of Eu^{3+} ion instead of Bi^{3+} ion transformed the structure from rhombohedral to orthorhombic at a concentration of x=0.2. The influences of oxygen vacancy and magnetoelectric coupling were reported to be at the maximum at a concentration of x=0.2 due to the structural distortion. This enhanced the dielectric constant, dielectric leakage and conductivity at this concentration, and the maximum value of dielectric constant reached was reported to be around 301.87. The dielectric constant value was reported to decrease with increase in the frequency. Similarly, the reduction in dielectric leakage with an increase in frequency was explained using Koop's phenomenological theory.[6,99] Enhanced dielectric- and saturation-magnetization of Eu-doped BFO are reported in Table 6 and they are very useful for application in the fabrication of potential devices in spintronics, nanoelectronics and for memory storage.

4.2.   *B-site doping*

The *B*-site substitutions are made by replacing the Fe^{3+} ions by other transition metal ions. Since the conduction band of BFO is related to the *d*-orbital state of Fe^{3+} ions, *B*-site substitutions can have a strong influence on the physical properties by changing the electronic structure near the Fermi level. The substitution may result in ordered structures of dopant ions or random distributions which are strongly related to the ionic radius of the dopant. Hence, *B*-site doping modifies the electronic and magnetic properties that may reduce the leakage currents.

Table 5.   Summary of reported Gd-doped BFO nanostructures.

Method of synthesis	Structure(s)	Reported significance	Source
Solid-state reaction route	Distorted rhombohedral structure to pseudocubic phase	Enhanced magnetization, magnetoelectric coupling and low activation energy values	Ref. 93
Solid-state reaction method	Rhombohedral phase to orthorhombic	Great enhancement in the remnant magnetization (M_r) and H_c values	Ref. 94
Sol–gel-derived route	Transition from rhombohedral to orthorhombic	Enhancement of remnant magnetization	Ref. 95
Sol–gel method	Rhombohedral to orthorhombic	Enhanced ferromagnetic character and magnetization values. Gd doping reduced the leakage current by four orders of magnitude	Ref. 96
Novel slow step sintering route	Rhombohedral structure to orthorhombic	Ferroelectric and ferromagnetic properties got enhanced	Ref. 97

Table 6.   Summary of reported Eu-doped BFO nanostructures.

Method of synthesis	Structure(s)	Reported significance	Source
Sol–gel method	Distorted rhombohedral structure	High dielectric constant	Ref. 100
Solid-state reaction method	Rhombohedrally distorted perovskite structure	Improved dielectric properties, decreased optical bandgap	Ref. 101
Solid-state reaction method	Rhombohedral	Saturated P–E loops, reduced leakage current	Ref. 102
Sol–gel method	Rhombohedral	Enhanced magnetization	Ref. 103

4.2.1. *Ni-doped BFO nanostructures*

Several studies have been devoted to improving the multiferroic properties of $BiFeO_3$ with the reduction of size to nanoscale on improvement of the magnetic properties of $BiFeO_3$. This can be done through cation substitution realized by *B*-site (Fe-site) doping, with the magnetic ions of Ni[104–106] for enhancing magnetization. The Ni atom was considered as a candidate for the enhancement of magnetic properties due to the fact that its ion radius is similar for substitution which may be attributed to the size effect of nanostructures and their magnetic properties.

BFO and Ni-doped BFO nanoparticles were reported to be successfully synthesized via the low-temperature sol–gel method by Nadeem *et al*.[107] The remanent polarization of the Ni-doped BFO sample was reported to be 19.43 times higher than that of pristine BFO. The Ni doping leads to a significant improvement in the dielectric, magnetic and ferroelectric properties of BFO. The reported increase in the magnetization may be due to the suppression of spin spiral structure because of the nanosized particles. Both the dielectric constant and the loss tangent were reported to decrease with increase in frequency because of the possible interfacial/space-charge polarization phenomenon. The strength of the dielectric constant depends on the space charge that is associated with the density of oxygen vacancies.[107] The leakage current was reported to decrease with increase in the doping concentration due to the suppression of impurity phases.[107] Hence, Ni doping was reported to be effective in improving

the dielectric as well as multiferroic properties of BFO. The material characteristics of these reported samples could be highly useful in various device applications.

Betancourt-Cantera *et al*.[108] synthesized $BiFe_{1-x}Ni_xO_3$ ($0 \leq x \leq 0.5$) by high-energy ball-milling method and the structural and multiferroic properties were studied and reported. Behavior modifications of electrical conductivity, permittivity and dielectric loss versus frequency that are related to the crystal structure transformations with increased nickel concentrations were studied and reported. The dielectric loss and conductivity were enhanced due to the oxygen vacancy generation.

($BiFe_{1-x}Ni_xO_3$ ($x = 0$, 0.05, 0.1, 0.2, 0.3) nanoparticles were successfully synthesized by a simple solution method by Khajonrit *et al*.[109] in 2017. The increasing of Ni content with the decreasing of crystallite size was reported to improve magnetization. Moreover, to study the electrochemical properties, the samples were fabricated as electrodes. The increasing of Ni content decreased the specific capacitances. But the $BiFe_{0.95}Ni_{0.05}O_3$ electrodes with a small mesopore size were reported to exhibit an enhanced capacity retention as high as 82% after 500 cycles, which can be considered as a good candidate for use in supercapacitors.

Kumar and Yadav[106] studied and reported the structural, magnetic, magnetocapacitance and dielectric properties of $BiFe_{1-x}Ni_xO_3$ nanoceramics prepared by the sol–gel method. Dielectric constant was found to decrease with increase in frequency. The magnetization and dielectric constant were

reported to be enhanced in the quenched samples than those of the normal sintered sample. Low variation in magnetocapacitance with an applied magnetic field was reported. The reported magnetization of the sample was 3.2 emu/g and the dielectric constant at room temperature was 930.

4.2.2. *Mn-doped BFO nanostructures*

Among the *B*-site substitutions, the Mn substitutions in BFO were known to enhance the ferromagnetic as well as ferroelectric orders by their possible existence in both Mn^{3+} and Mn^{4+} valence states[110] and they are dependent strongly on the dynamics of domain walls in multiferroic materials.[111–113]

Ghahfarokhi *et al*. reported the structural, magnetic, dielectric and optical properties of Mn-doped BFO nanoparticles prepared by sol–gel method. The particles showed decrease in their crystallite size with increase in the doping concentration. The particles exhibited strong ferromagnetic properties and high bandgap with increased doping concentration. The dielectric constant and dielectric loss decreased with increased electrical conductivity by doping.[114]

Multiferroic Mn-doped BFO nanoparticles were synthesized using sol–gel auto-combustion method by Dhanalakshmi *et al*.[115] Manganese was found to reduce the oxygen vacancies due to its multivalent states due to which the electrical and magnetic properties can be reduced. It was reported that the dielectric and ferromagnetic properties were enhanced along with the magnetoelectric coupling and hence they can be used in multiferroic device applications. The relatively high dielectric constant ε' of the Mn-doped BFO with increasing concentration of Mn confirmed the space-charge polarization.

The structural phase transition and surface morphology changes lead to enhanced magnetic properties in Mn-doped BFO sample prepared using the standard coprecipitation method by Awasthi *et al*.[116] The enhancement of ferroelectric behavior and suppression of the leakage current density due to Mn doping were reported. The electrical conductivity of the doped samples was reported to be enhanced.[116]

4.2.3. *Cr-doped BFO nanostructures*

According to Kanamori rule,[117–119] the spin coupling of Fe-d^5–O–Cr-d^3 bond is likely to develop ferromagnetic ordering in the perovskite while the stereo-active $6s^2$ lone pair is understood to give rise to ferroelectricity.

Sinha *et al*. synthesized Cr-doped BFO nanoparticles by the sol–gel method.[120] The increase in Cr doping concentration resulted in decrease in grain size with enhanced dielectric properties and suppressed leakage current. In the reported work, the value of P_r increased by nearly three times in pure BFO nanoparticles, which can be attributed to a reduction in the leakage current. It was reported that owing to the enhanced ferroelectric and magnetic properties, these materials are used to design efficient memory devices. Due to their

absorption property in the visible spectra, they are used in photocatalytic applications.

Cr-doped nanoceramics synthesized using sol–gel route by Kumar and Yadav showed enhanced magnetization and magnetocapacitance.[121] The dielectric constant and dielectric loss were found to exhibit the same behaviors with increasing frequency as reported in previous reports. The dielectric constant of a material can be influenced by various factors. As reported for Cr-doped BFO nanoceramics,[121] the change of dielectric constant (ε) by the variation of magnetic field can be induced not only by magnetoelectric coupling effect but also by other factors such as the magnetostriction effect, which occurs due to the change in lattice parameters by applying the magnetic field. The change in lattice parameters results in the change in shape or dimension of the particle and thereby affecting the dielectric properties. Similar findings were reported by Kumari *et al*.[6] and Sheoran *et al*.[84]

4.2.4. *Ti-doped BFO nanostructures*

The existence of mixed valence state of Fe ions (Fe^{2+}/Fe^{3+}), existence of oxygen vacancies and the existence of spiral spin modulation in BFO system are some of the problems due to which it is difficult to derive the ferromagnetism with net magnetization.[36] Ti doping is considered to be one of the most effective methods to overcome the above-mentioned problems because Ti^{4+} ions can reduce the concentrations of oxygen vacancies and Fe^{2+} ions in BFO ceramics, and thus the dielectric loss and conductivity could be reduced.[122–124] Also, it enhances the magnetization because it breaks the balance between two adjacent antiparallel spin lattices of Fe^{3+} ions.

The Ti-doped BFO nanoceramics synthesized by Tian *et al*.[125] provided a proof that the polarization can be switched on applying the electric field and hence, the ferroelectric domains can also be controlled in nanoscale. With Ti doping, large remanent polarization (P_r) and maximum polarization (P_{max}) were observed, which are significantly larger than those of BFO ceramics.

4.3. *Oxygen-site substitution*

It is well known that BFO loses oxygen, resulting in the formation of both bulk and surface vacancies in O-site substitution. The presence of such oxygen vacancies changes both the electrical and magnetic properties of BFO. Seidel *et al*.[126] have reported the impact on the electrochemical properties of $B_{0.9}Ca_{0.1}FeO_{3–0.05}$ due to the oxygen vacancies.

4.4. *BFO thin films for the enhancement of dielectric properties*

BFO thin films have attracted more and more attention due to excellent ferroelectric performance.[127] Recently, Wang *et al*.[128] have reported BFO thin film on the SRO/STO

substrates with high remnant polarization. The structure of epitaxial BFO film is closely related to the thickness of the film and the epitaxial strain on different substrates. Further, doping of other elements affects the structure of the BFO thin films.[129]

BFO thin films usually suffer from large leakage current due to the oxygen vacancies and Fe^{2+} ions in the samples,[130,131] so interface effects play a notable role in the BFO thin-film capacitors. Lee *et al.* have found that the film–electrode interfaces greatly affect the leakage current of BFO thin films.[132] A high coercive field was reported in the BFO film on LNO, which had probably originated from the small grain size of the BFO films. Leakage current, which is one of the conventional problems, was reported to be greatly reduced with remarkable improvement in the interface, chemical homogeneity, crystallinity and surface roughness of the BFO film.[132]

Dielectric properties of the BFO thin films were investigated in In/BFO/LSMO capacitor configuration by Liu *et al.*[133] The capacitance was reported to decrease with increasing bias voltage and frequency at low frequencies. It was reported that the interfacial polarization leads to the strong dependences of capacitance of the BFO thin-film capacitors on frequency and bias voltage at low frequencies.

Shah *et al.* prepared bismuth iron oxide $(Bi_{1-x}K_xFeO_3)$ thin films using sol–gel and the spin coating methods.[134] It was reported that ferromagnetic behavior arises in doped $BiFeO_3$ films due to suppression of helical spin structure. The presence of dopant atoms in BFO host lattice was reported to reduce the number of oxygen vacancies,[135] thus reducing

the conductivity of the films and consequently increasing the dielectric constant up to a dopant concentration of 0.15 wt%.

The relationships of structures, surface morphologies as well as magnetic properties of codoped thin films prepared using the sol–gel technique were systematically studied and reported by Bai *et al.*[136] The reported enhancements of M_s and M_r were mainly derived from the decrease of oxygen defects concentration, the denser agglomerations, the enhanced superexchange interaction and the breakdown of spiral spin structure. These results demonstrated that Co^{3+} doping in BFO thin films is an effective method to improve their magnetic characteristics. Codoped BFO thin films are considered to have better application prospects in multiferroic memory devices, information storage and magnetic switch devices at room temperature.

Yan *et al.*[137] fabricated the ruthenium (Ru)-doped BFO (BFRO) films by the pulsed laser deposition system. The leakage current of the BFRO film was reported to decrease. A better coupling between ferroelectric ordering and ferromagnetic ordering had been reported via doping Ru ions into the Fe site of BFO. The improved ferroelectric, ferromagnetic and dielectric properties of the BFRO film were ascribed to the reduced concentrations of defects and defect dipole complex, valence effect of Ru ions and a different domain behavior. The enhanced magnetic properties of ruthenium-doped BFO are reported to arise due to the distorted spin cycloid and canting angle of Fe ions in the Ru-doped BFO film. The decrease in oxygen vacancies corresponds to the lower leakage current densities.[137]

Table 7.   Summary of various reported nanocomposites.

S. no.	Nanocomposite	Method	Size	Reported significance	Source
1	$BiFeO_3$–$PbTiO_3$	Solid-state reaction	0.2–0.8 μm	Reduced activation energy	Ref. 142
2	BFO–NFO	Sol–gel	10–7 nm	Improved dielectric constant	Ref. 143
3	$BiFeO_3$–$CoFe_2O_4$	Sol–gel	15–25 nm	Increase in magnetization	Ref. 144
4	$BiFeO_3$–$MnFe_2O_4$	Sol–gel auto-combustion	60–90 nm	Enhanced dielectric properties	Ref. 145
5		Sol–gel auto-combustion	700–1200 μm	Enhanced ferroelectric and ferromagnetic properties	Ref. 146
6	$BiFeO_3$–$MgFe_2O_4$	Sol–gel	30–50 nm	Enhanced magnetic, dielectric and ME responses	Ref. 147
7	$BiFeO_3$–$ZnFe_2O_4$	Citrate sol–gel precursor method	Size of $BiFeO_3$ is 26 nm and size of $ZnFe_2O_4$ is 21 nm	Improved ME coupling effect	Ref. 148
8	$BiFeO_3$–$CoFe_2O_4$ (core–shell nanocomposites)	Sol–gel auto-combustion method	Size of the cores is 10–35 nm and size of the shells is 40–100 nm	Increase in saturation magnetization	Ref. 149
9	$BiFeO_3$–$CoFe_2O_4$ (tubular interfaces)	Magnetron sputtering	7- and 9-nm tall with edge lengths of less than 120 nm	Enhanced conductivity	Ref. 150
10	$BiFeO_3$–$BaTiO_3$ (disc-shaped)	Solid-state reaction method	Diameter ~10 mm with 1 mm of thickness	Thermally stable dielectric and energy storage properties	Ref. 151
11	$BiFeO_3$–Fe_3O_4 (irregular shape)	Sol–gel	Size of BFO in the range of 43–51 nm and size of Fe_3O_4 in the range of 10–12 nm	Increased photocurrent density and photoemission	Ref. 152

La-doped BFO thin films were grown on $Pt/TiO_2/SiO_2/Si$ substrate using pulsed laser deposition by Yan *et al.* in 2010.[138] With La doping, highly enhanced ferroelectric properties with great remnant polarization (P_r) and decreased leakage current density were reported. The leakage current density was reported to be reduced up to two orders of magnitude for La-doped samples when compared with BFO.[138] An enhancement in magnetic property was also reported, ascribed to spatial homogenization of the spin arrangement. La dopant significantly enhanced the dielectric constant from 190 to 290 at 1 kHz.

4.5. *BFO as multiferroic composites*

Magnetoelectric materials can be divided into two categories: single phases and composites. Different ferroic properties can be combined in the same phase of a crystal, provided that the right symmetry of the ferroic phase and the appropriate pair of the prototype phase point group–ferroic phase point group were reported.[139,140] The composites are mixtures of ferroelectric and ferromagnetic materials, that offer a much higher magnetoelectric coefficient than single phases but the magnetoelectric coupling is merely restricted to interfaces.[141]

The composites $Bi_{0.5}Dy_xFe_{1-x}O_{3-0.5}PbTiO_3$ ($x=0$, 0.05, 0.10, 0.15, 0.20) were prepared by a high-temperature solid-state reaction technique by Mohanty *et al.*[142] X-ray analysis confirmed that the composites had a tetragonal crystal structure. The average grain size was reported to be in the range of 0.2–0.8 μm. The dielectric constant was reported to be increased with increase in the Dy concentration. The increased value of bulk polarization was reported either due to charge reordering (electronic ferroelectrics) in which the existing charge distribution reordering is in a nonsymmetric fashion to induce electric polarization or through structural transition or magnetic ordering.[142]

The variation of AC conductivity of the composites as a function of temperature was reported to exhibit Arrhenius type of electrical conductivity. The composites showed negative temperature of coefficient of resistance. The activation energy was reported to be of small value and increased slowly with increase in the concentration, due to the strong intra-atomic Coulomb repulsion between the *f–f* electrons.

Kaur and Verma[143] synthesized the nanocomposites of $Bi_{1-x}FeO_{3-x}NiFe_2O_4$ for $x=$ 0.2, 0.4 and 0.6 by the sol–gel technique and its various properties were studied and reported. The average particle size was reported to be decreasing from 10 nm to 7 nm as the concentration of $NiFe_2O_4$ increases. The saturation magnetization increased up to 10 emu/g on increasing the $NiFe_2O_4$ concentration. The dielectric constant was reported to increase with increase in the concentration of nickel ferrite. It was confirmed that coercivity increased slowly with decrease of temperature in the nickel ferrite–bismuth ferrite composite.[143] The polarization values were found to decrease as a result of intrinsic contribution.

Das *et al.*[144] prepared the $BiFeO_3$–$CoFe_2O_4$ nanocomposites with the nominal formula of $Co_xFe_2O_{4-(1-x)}BiFeO_3$ ($x=0.2, 0.3, 0.4$), by using the sol–gel method. TEM images exhibited that particle sizes of the prepared samples are in the 15–25-nm range. Room-temperature *M–H* hysteresis loops of nanocomposites have reported substantial increment in magnetization value in comparison with that of the pristine BFO and this value is found to increase with the increase in CFO content. The dielectric constant versus temperature curves of all samples exhibited increment of dielectric constant with increasing temperature. The variation in dielectric constant with applied magnetic field (magnetocapacitance) confirmed the presence of magnetoelectric coupling. Hence, both magnetic and magnetoelectric properties were enhanced. The change in capacitance in the presence of magnetic field is often known as magnetocapacitance which is a measure of ME coupling in a material. Hence, magnetocapacitance of a material generally arises from both the intrinsic and extrinsic effects. A positive magnetocapacitance effect is reported due to the increase in MC values with increasing magnetic field.

$(BFO)_{1-x}(Fe_3O_4)_x$ nanocomposites synthesized by dispersion of Fe_3O_4 nanoparticles into sol–gel-synthesized BFO were reported by Baqiah *et al.*[152] The bandgap decreased with increase in the doping concentration. The photocurrent density was reported to be enhanced. Modulations in physical properties were observed in the BFO–Fe_3O_4 nanocomposite samples, which make it a potential material for photoenergy conversion applications.[152]

It is known that structure/phase degeneracy in solids is crucial in modern functional material design. The energy degeneracy of different polar structures with varying symmetries at the phase boundary gives rise to significant reduction of polarization anisotropy as well as domain wall energy, which further brings about the formation of nanodomains.

In a recent study, Pan *et al.*[153] reported that the coexistence of rhombohedral and tetragonal nanodomains embedded in a cubic matrix achieved simultaneously high polarization and low loss. This is associated with the enhanced relaxor property. The polarization was reported to be enhanced whereas the dissipation energy was decreased with suppressed dielectric loss over the wide temperature and frequency ranges.[153] Hence, the polymorphic nanodomain design improved the overall dielectric energy storage performance and therefore can be used in a number of functional applications.

The polymorphic nanodomain approach by Pan *et al.* may also be applied in AFE to eliminate the polarization hysteresis and achieve high efficiency. The polymorphic nanodomain contributed to the high energy density of 112 J/cm³ with a discharge/charge efficiency of 80%. Similarly, Yang *et al.*[154] in 2020 designed a flexible BFMO–SBT thin-film capacitor that exhibited a high recoverable energy storage density (61 J/cm³) and a high efficiency of 75% combined with a fast discharging rate of 23.5 μs.

5   Summary and Outlook

Multiferroic nanomaterials have attracted great interest due to the simultaneous presence of two or more properties such as ferroelectricity, ferromagnetism and ferroelasticity that promise wide applications in multifunctional, low-power-consumption and eco-friendly devices. BFO exhibits both (A)FM and FE properties at room temperature and plays a significant role in multiferroic system. In this review, the development of BFO nanomaterials, including their morphology, structure and properties for energy applications, was systematically analyzed and discussed.

This review presents an overview of the dielectric properties of BFO nanomaterials, thin films and BFO nanocomposites which were prepared using various synthesis techniques exhibiting unique properties like ferroelectricity, ferromagnetization, magnetoelectric coupling, remnant polarization, piezoelectricity, enhanced photocurrent and current density. It was observed that progress has been made in each site of doping, thereby exploring various multiferroic properties. The size, shape and structural changes contribute to the variation of magnetoelectric property in multiferroic materials. The leakage problem of the multiferroic materials was reported to be decreased as a result of both *A*-site and *B*-site doping.

It was analyzed that some interesting improvements and achievements have been made in the energy storage and photovoltaic applications, but there are still few issues that have to be resolved in order to exhibit their maximum performance. The aspects to be highlighted from this review are summarized as follows.

A-site substitution reports were reviewed and it was found to influence the band structure and properties dependent on ionic size of the substitution elements. Increase in Ca/Pb doping reduced the leakage current and dielectric loss. Rare-earth-doped BFO enhanced magnetization and improved the dielectric properties. Cation-substituted *B*-site (Fe-site) doping with increased concentrations of the magnetic ions of Ni, Cr, Mn and Ti was reviewed, and enhanced magnetic properties with decreased crystallite size were reported as suitable candidates for supercapacitor applications. Enhanced dielectric properties of BFO thin films due to thickness and dopants of film and epitaxial strains on the different substrates were studied. BFO composites were reviewed and reported to offer higher magnetoelectric effect. The spontaneous polarization and remanent polarization of BFO are key parameters for energy storage. Further, the enhancement of magnetic properties is reported at the expense of electrical performances and its impacts on energy storage properties are also reviewed. The discussions of electric and magnetic properties are related to each other and their impacts on BFO-based energy storage systems are summarized in few notable reports. This review acts as an update and encourages more researches to push on the development of BFO nanomaterials for energy applications in the future.

References

[1] T. M. Correia, M. McMillen, M. K. Rokosz, P. M. Weaver, J. M. Gregg, G. Viola and M. G. Cain, A lead-free and high-energy density ceramic for energy storage applications, *J. Am. Ceram. Soc.* **96**, 2699 (2013), doi:10.1111/jace.12508.

[2] X. Hao, A review on the dielectric materials for high energy-storage application, *J. Adv. Dielectr.* **03**, 1330001 (2013), doi:10.1142/s2010135x13300016.

[3] Y. Suzuki, T. S. Suzuki, K. Hirao, T. Tsuchiya, H. Nagata and J. S. Cross, *Advanced Ceramic Technologies & Products* (Springer Science & Business Media, Berlin, 2012).

[4] R. E. Smallman and R. J. Bishop, *Modern Physical Metallurgy and Materials Engineering* (Elsevier, Amsterdam, 1999).

[5] J. Wang, H. Zheng, Z. Ma, S. Prasertchoung, M. Wuttig, R. Droopad, J. Yu, K. Eisenbeiser and R. Ramesh, Epitaxial $BiFeO_3$ thin films on Si, *Appl. Phys. Lett.* **85**, 2574 (2004), doi:10.1063/1.1799234.

[6] B. Kumari, P. R. Mandal and T. K. Nath, Magnetic, magnetocapacitance and dielectric properties of $BiFeO_3$ nanoceramics, *Adv. Mater. Lett.* **5**, 84 (2014), doi:10.5185/amlett.2013.fdm.36.

[7] K. Ueda, H. Tabata and T. Kawai, Coexistence of ferroelectricity and ferromagnetism in $BiFeO_3$–$BaTiO_3$ thin films at room temperature, *Appl. Phys. Lett.* **75**, 555 (1999), doi:10.1063/1.124420.

[8] M. Mahesh Kumar, A. Srinivas and S. V. Suryanarayana, Structure property relations in $BiFeO_3$/$BaTiO_3$ solid solutions, *J. Appl. Phys.* **87**, 855 (2000), doi:10.1063/1.371953.

[9] T. Durga Rao, T. Karthik and S. Asthana, Investigation of structural, magnetic and optical properties of rare earth substituted bismuth ferrite, *J. Rare Earths* **31**, 370 (2013), doi:10.1016/S1002-0721(12)60288-9.

[10] V. A. Khomchenko, I. O. Troyanchuk, M. I. Kovetskaya, M. Kopcewicz and J. A. Piaxão, Effect of Mn substitution on crystal structure and magnetic properties of $Bi_{1-x}Pr_xFeO_3$ multiferroics, *J. Phys. D, Appl. Phys.* **45**, 045302 (2012), doi:10.1088/0022-3727/45/4/045302.

[11] V. V. Lazenka, G. Zhang, J. Vanacken, I. I. Makoed, A. F. Ravinski and V. V. Moshchalkov, Structural transformation and magnetoelectric behavior in $Bi_{1-x}Gd_xFeO_3$ multiferroics, *J. Phys. D, Appl. Phys.* **45**, 125002 (2012), doi:10.1088/0022-3727/45/12/125002.

[12] Y.-J. Wu, J. Zhang, X.-K. Chen and X.-J. Chen, Phase evolution and magnetic property of $Bi_{1-x}Ho_xFeO_3$ powders, *Solid State Commun.* **151**, 1936 (2011), doi:10.1016/j.ssc.2011.09.020.

[13] H. Y. Dai, H. Z. Liu, J. F. Du, T. Li, R. Z. Xue and Z. P. Chen, Effect of sintering temperature on the microstructure, electrical, and magnetic properties of $Bi_{0.85}Eu_{0.15}FeO_3$ ceramics, *J. Supercond. Nov. Magn.* **27**, 2105 (2014), doi:10.1007/s10948-014-2558-4.

[14] A. Kumar and D. Varshney, Crystal structure refinement of $Bi_{1-x}Nd_xFeO_3$ multiferroic by the Rietveld method, *Ceram. Int.* **38**, 3935 (2012), doi:10.1016/j.ceramint.2012.01.046.

[15] X. Qi, J. Dho, R. Tomov, M. G. Blamire and J. L. MacManus-Driscoll, Greatly reduced leakage current and conduction mechanism in aliovalent-ion-doped $BiFeO_3$, *Appl. Phys. Lett.* **86**, 062903 (2005), doi:10.1063/1.1862336g.

[16] S. Layek, S. Saha and H. C. Verma, Preparation, structural and magnetic studies on $BiFe_{1-x}Cr_xO_3$ (*x*=0.0, 0.05 and 0.1) multiferroic nanoparticles, *AIP Adv.* **3**, 032102 (2013), doi:10.1063/1.4799063.

[17] I. K. Battisha, I. S. A. Farag, M. Kamal, M. A. Ahmed, E. Girgis, H. A. El Meleegi and F. El Desouki, Dielectric and magnetic properties of nano-structure $BiFeO_3$ doped with different concentrations of Co ions prepared by sol-gel method, *New J. Glass Ceram.* **5**, 59 (2015), doi:10.4236/njgc.2015.53008.

[18] A. T. Raghavender and N. H. Hong, Effects of Mn doping on structural and magnetic properties of multiferroic $BiFeO_3$ nanograins made by sol-gel method, *J. Magn.* **16**, 19 (2011), doi:10.4283/JMAG.2011.16.1.019.

[19]B. Peng, Q. Zhang, X. Li, T. Sun, H. Fan, S. Ke, M. Ye, Y. Wang, W. Lu, H. Niu, J. F. Scott, X. Zeng and H. Huang, Giant electric energy density in epitaxial lead-free thin films with coexistence of ferroelectrics and antiferroelectrics, *Adv. Electron. Mater.* **1**, 1500052 (2015), doi:10.1002/aelm.201500052.

[20]N. H. Fletcher, A. D. Hilton and B. W. Ricketts, Optimization of energy storage density in ceramic capacitors, *J. Phys. D, Appl. Phys.* **29**, 253 (1996), doi:10.1088/0022-3727/29/1/037.

[21]X. Hao, A review on the dielectric materials for high energy-storage application, *J. Adv. Dielectr.* **03**, 1330001 (2013), doi:10.1142/S2010135X13300016.

[22]A. Chauhan, S. Patel, R. Vaish and C. R. Bowen, Anti-ferroelectric ceramics for high energy density capacitors, *Materials* **8**, 8009 (2015), doi:10.3390/ma8125439.

[23]R. Ramesh and N. A. Spaldin, *Nanoscience and Technology: A Collection of Reviews from Nature Journals*, ed. P. Rodgers, Chapter 3 (Nature Publishing Group and Macmillan Publishers, 2009), pp. 20–28, doi:10.1142/9789814287005_0003.

[24]H. Ishiwara, Impurity substitution effects in BiFeO3 thin films — From a viewpoint of FeRAM applications, *Curr. Appl. Phys.* **12**, 603 (2012), doi:10.1016/j.cap.2011.12.019.

[25]L. W. Martin, S. P. Crane, Y.-H. Chu, M. B. Holcomb, M. Gajek, M. Huijben, C.-H. Yang, N. Balke and R. Ramesh, Multiferroics and magnetoelectrics: Thin films and nanostructures, *J. Phys., Condens. Matter* **20**, 434220 (2008), doi:10.1088/0953-8984/20/43/434220.

[26]Y. E. Roginska, Y. Y. Tomashpo, Y. N. Venevtse, V. M. Petrov and G. S. Zhdanov, Nature of dielectric and magnetic properties of BeFeO$_3$, *Sov. Phys.-JETP* **23**, 47 (1966).

[27]S. V. Kiselev, R. P. Ozerov and G. S. Zhdanov, Detection of magnetic order in ferroelectric BiFeO$_3$ by neutron diffraction, *Sov. Phys. Dokl.* **7**, 742 (1963).

[28]J. R. Teague, R. Gerson and W. J. James, Dielectric hysteresis in single crystal BiFeO$_3$, *Solid State Commun.* **8**, 1073 (1970), doi:10.1016/0038-1098(70)90262-0.

[29]J. Wang, J. B. Neaton, H. Zheng, V. Nagarajan, S. B. Ogale, B. Liu, D. Viehland, V. Vaithyanathan, D. G. Schlom, U. V. Waghmare, N. A. Spaldin, K. M. Rabe, M. Wuttig and R. Ramesh, Epitaxial BiFeO$_3$ multiferroic thin film heterostructures, *Science* **299**, 1719 (2003), doi:10.1126/science.1080615.

[30]M. Ranjbar, M. E. Ghazi and M. Izadifard, Investigation of the annealing temperature effect on structural, morphology, dielectric and magnetic properties of BiFeO$_3$ nanoparticles, *Physica C* **549**, 73 (2018), doi:10.1016/j.physc.2018.02.052.

[31]A. K. Pradhan *et al.*, Magnetic and electrical properties of single-phase multiferroic BiFeO$_3$, *J. Appl. Phys.* **97**, 093903 (2005), doi:10.1063/1.1881775.

[32]S.-H. Lim, M. Murakami, J. H. Yang, S.-Y. Young, J. Hattrick-Simpers, M. Wuttig, L. G. Salamanca-Riba and I. Takeuchi, Enhanced dielectric properties in single crystal-like BiFeO$_3$ thin films grown by flux-mediated epitaxy, *Appl. Phys. Lett.* **92**, 012918 (2008), doi:10.1063/1.2831665.

[33]X. H. Zheng, P. J. Chen, N. Ma, Z. H. Ma and D. P. Tang, Synthesis and dielectric properties of BiFeO$_3$ derived from molten salt method, *J. Mater. Sci., Mater. Electron.* **23**, 990 (2012), doi:10.1007/s10854-011-0533-4.

[34]R. Safi and H. Shokrollahi, Physics, chemistry and synthesis methods of nanostructured bismuth ferrite (BiFeO$_3$) as a ferroelectro-magnetic material, *Prog. Solid State Chem.* **40**, 6 (2012), doi:10.1016/j.progsolidstchem.2012.03.001.

[35]R. Mazumder, P. Sujatha Devi, D. Bhattacharya, P. Choudhury, A. Sen and M. Raja, Ferromagnetism in nanoscale BiFeO$_3$, *Appl. Phys. Lett.* **9**, 062510 (2007), doi:10.1063/1.2768201.

[36]T.-J. Park, G. C. Papaefthymiou, A. J. Viescas, A. R. Moodenbaugh and S. S. Wong, Size-dependent magnetic properties of single-crystalline multiferroic BiFeO$_3$ nanoparticles, *Nano Lett.* **7**, 766 (2007), doi:10.1021/nl063039w.

[37]L. Zhang, X.-F. Cao, Y.-L. Ma, X.-T. Chen and Z.-L. Xue, Polymer-directed synthesis and magnetic property of nanoparticles-assembled BiFeO$_3$ microrods, *J. Solid State Chem.* **183**, 1761 (2010), doi:10.1016/j.jssc.2010.05.029.

[38]T.-J. Park, Y. Mao and S. S. Wong, Synthesis and characterization of multiferroic BiFeO$_3$ nanotubes, *Chem. Commun.* **2004**, 2708 (2004), doi:10.1039/b409988e.

[39]J. Wei, D. Xue and Y. Xu, Photoabsorption characterization and magnetic property of multiferroic BiFeO$_3$ nanotubes synthesized by a facile sol–gel template process, *Scr. Mater.* **58**, 45 (2008), doi:10.1016/j.scriptamat.2007.09.001.

[40]Y. Wang, G. Xu, L. Yang, Z. Ren, X. Wei, W. Weng, P. Du, G. Shen and G. Han, Hydrothermal synthesis of single-crystal bismuth ferrite nanoflakes assisted by potassium nitrate, *Ceram. Int.* **35**, 1285 (2009), doi:10.1016/j.ceramint.2008.04.016.

[41]D. P. Dutta, O. D. Jayakumar, A. K. Tyagi, K. G. Girija, C. G. S. Pillai and G. Sharma, Effect of doping on the morphology and multiferroic properties of BiFeO$_3$ nanorods, *Nanoscale* **2**, 1149 (2010), doi:10.1039/c0nr00100g.

[42]F. Gao, X. Chen, K. Yin, S. Dong, Z. Ren, F. Yuan, T. Yu, Z. Zou and J.-M. Liu, Visible-light photocatalytic properties of weak magnetic BiFeO$_3$ nanoparticles, *Adv. Mater.* **19**, 2889 (2007), doi:10.1002/adma.200602377.

[43]F. Gao *et al.*, Preparation and photoabsorption characterization of BiFeO$_3$ nanowires, *Appl. Phys. Lett.* **89**, 102506 (2006), doi:10.1063/1.2345825.

[44]S. H. Xie *et al.*, Nanocrystalline multiferroic BiFeO$_3$ ultrafine fibers by sol-gel based electrospinning, *Appl. Phys. Lett.* **93**, 222904 (2008), doi:10.1063/1.3040010.

[45]U. A. Joshi, J. S. Jang, P. H. Borse and J. S. Lee, Microwave synthesis of single-crystalline perovskite BiFeO$_3$ nanocubes for photoelectrode and photocatalytic applications, *Appl. Phys. Lett.* **92**, 242106 (2008), doi:10.1063/1.2946486.

[46]W. Eerenstein, N. D. Mathur and J. F. Scott, Multiferroic and magnetoelectric materials, *Nature* **442**, 759 (2006), doi:10.1038/nature05023.

[47]M. Fiebig, T. Lottermoser, D. Fröhlich, A. V. Goltsev and R. V. Pisarev, Observation of coupled magnetic and electric domains, *Nature* **419**, 818 (2002), doi:10.1038/nature01093.

[48]M. I. Danilkevitch and I. I. Makoed, Dielectric properties of spinel, garnet and perovskite oxides, *Phys. Status Solidi B* **222**, 541 (2000), doi:10.1002/1521-3951(200011)222:2<541::AID-PSSB541>3.0.CO;2-0.

[49]D. Kothari, V. Raghavendra Reddy, A. Gupta, V. Sathe, A. Banerjee, S. M. Gupta and A. M. Awasthi, Multiferroic properties of polycrystalline Bi$_{1-x}$Ca$_x$FeO$_3$, *Appl. Phys. Lett.* **91**, 202505 (2007), doi:10.1063/1.2806199.

[50]H. Wu and X. Zhu, Microstructures, magnetic, and dielectric properties of Ba-doped BiFeO$_3$ nanoparticles synthesized via molten salt route, *J. Am. Ceram. Soc.* **102**, 4698 (2019), doi:10.1111/jace.16348.

[51]W. Liu, G. Tan, X. Xue, G. Dong and H. Ren, Structure transition and enhanced ferroelectric properties of (Mn, Cr) co-doped BiFeO$_3$ thin films, *J. Mater. Sci., Mater. Electron.* **24**, 4827 (2013), doi:10.1007/s10854-013-1482-x.

[52]R. Das and K. Mandal, Magnetic, ferroelectric and magnetoelectric properties of Ba-doped BiFeO$_3$, *J. Magn. Magn. Mater.* **324**, 1913 (2012), doi:10.1016/j.jmmm.2012.01.022.

[53]M. Hasan, M. A. Hakim, M. A. Basith, Md. S. Hossain, B. Ahmmad, M. A. Zubair, A. Hussain and Md. F. Islam, Size dependent magnetic and electrical properties of Ba-doped nanocrystalline BiFeO$_3$, *AIP Adv.* **6**, 035314 (2016), doi:10.1063/1.4944817.

[54]C. Yang, J.-S. Jiang, F.-Z. Qian, D.-M. Jiang, C.-M. Wang and W.-G. Zhang, Effect of Ba doping on magnetic and dielectric properties of nanocrystalline $BiFeO_3$ at room temperature, *J. Alloys Compd.* **507**, 29 (2010), doi:10.1016/j.jallcom.2010.07.193.

[55]P. Singh and J. H. Jung, Effect of oxygen annealing on magnetic, electric and magnetodielectric properties of Ba-doped $BiFeO_3$, *Physica B* **405**, 1086 (2010), doi:10.1016/j.physb.2009.11.007.

[56]R. Mahbub, T. Fakhrul, Md. F. Islam, M. Hasan, A. Hussain, M. A. Matin and M. A. Hakim, Structural, dielectric, and magnetic properties of Ba-doped multiferroic bismuth ferrite, *Acta Metall. Sin. (Engl. Lett.)* **28**, 958 (2015), doi:10.1007/s40195-015-0279-8.

[57]R. Mazumder and A. Sen, Effect of Pb-doping on dielectric properties of $BiFeO_3$ ceramics, *J. Alloys Compd.* **475**, 577 (2009), doi:10.1016/j.jallcom.2008.07.082.

[58]I. Ghafoor, S. A. Siddiqi, S. Atiq, S. Riaz and S. Naseem, Sol–gel synthesis and investigation of structural, electrical and magnetic properties of Pb doped $La_{0.1}Bi_{0.9}FeO_3$ multiferroics, *J. Sol-Gel Sci. Technol.* **74**, 352 (2014), doi:10.1007/s10971-014-3517-z.

[59]G. L. Yuan and S. W. Or, Multiferroicity in polarized single-phase $Bi_{0.875}Sm_{0.125}FeO_3$ ceramics, *J. Appl. Phys.* **100**, 024109 (2006), doi:10.1063/1.2220642.

[60]P. Uniyal and K. L. Yadav, Pr doped bismuth ferrite ceramics with enhanced multiferroic properties, *J. Phys., Condens. Matter* **21**, 405901 (2009), doi:10.1088/0953-8984/21/40/405901.

[61]X. Zhang, Y. Sui, X. Wang, J. Tang and W. Su, Influence of diamagnetic Pb doping on the crystal structure and multiferroic properties of the $BiFeO_3$ perovskite, *J. Appl. Phys.* **105**, 07D918 (2009), doi:10.1063/1.3079770.

[62]J. J. Ge, X. B. Xue, G. F. Cheng, M. Yang, B. You, W. Zhang, X. S. Wu, A. Hu, J. Du, S. J. Zhang, S. M. Zhou, Z. Wang, B. Yang and L. Sun, Nonmonotonic variation of magnetization in $Bi_{0.8}La_{0.2-x}Pb_xFeO_3$ ($0 \le x \le 0.2$) multiferroics, *J. Magn. Magn. Mater.* **324**, 200 (2012), doi:10.1016/j.jmmm.2011.08.010.

[63]V. A. Khomchenko *et al.*, Effect of diamagnetic Ca, Sr, Pb, and Ba substitution on the crystal structure and multiferroic properties of the $BiFeO_3$ perovskite, *J. Appl. Phys.* **103**, 024105 (2008), doi:10.1063/1.2836802.

[64]Reetu, A. Agarwal, S. Sanghi and Ashima, Rietveld analysis, dielectric and magnetic properties of Sr and Ti codoped $BiFeO_3$ multiferroic, *J. Appl. Phys.* **110**, 073909 (2011), doi:10.1063/1.3646557.

[65]K. W. Wagner, Zur theorie der unvollkommenen dielektrika, *Ann. Phys.* **40**, 817 (1913).

[66]J. R. Sahu and C. N. R. Rao, Beneficial modification of the properties of multiferroic $BiFeO_3$ by cation substitution, *Solid State Sci.* **9**, 950 (2007), doi:10.1016/j.solidstatesciences.2007.06.006.

[67]B. Bhushan, A. Basumallick, N. Y. Vasanthacharya, S. Kumar and D. Das, Sr induced modification of structural, optical and magnetic properties in $Bi_{1-x}Sr_xFeO_3$ (x = 0, 0.01, 0.03, 0.05 and 0.07) multiferroic nanoparticles, *Solid State Sci.* **12**, 1063 (2010), doi:10.1016/j.solidstatesciences.2010.04.026.

[68]X. Yuan, L. Shi, J. Zhao, S. Zhou, Y. Li, C. Xie and J. Guo, Sr and Pb co-doping effect on the crystal structure, dielectric and magnetic properties of $BiFeO_3$ multiferroic compounds, *J. Alloys Compd.* **708**, 93 (2017), doi:10.1016/j.jallcom.2017.02.288.

[69]C. Ehssalde and J. Raves, Ferroelectric ceramics: Defects and dielectric relaxations, *J. Mater. Chem.* **11**, 1957 (2001), doi:10.1039/b010117f.

[70]C. A. Wang, H. Z. Pang, A. H. Zhang, M. H. Qin, X. B. Lu, X. S. Gao, M. Zeng and J. M. Liu, Room temperature multiferroic and magnetodielectric properties in Sm and Sc co-doped

$BiFeO_3$ ceramics, *J. Phys. D, Appl. Phys.* **48**, 395302 (2015), doi:10.1088/0022-3727/48/39/395302.

[71]X. Yuan, L. Shi, J. Zhao, S. Zhou, J. Guo, S. Pan, X. Miao and L. Wu, Tuning ferroelectric, dielectric, and magnetic properties of $BiFeO_3$ ceramics by Ca and Pb co-doping, *Phys. Status Solidi B* **256**, 1800499 (2018), doi:10.1002/pssb.201800499.

[72]W. D. Judge, Z. W. Xiao and G. J. Kipouros, *Rare Metal Technology 2017*, eds. H. Kim, S. Alam, N. Neelameggham, H. Oosterhof, T. Ouchi and X. Guan, The Minerals, Metals & Materials Series, Chapter 4 (Springer, Cham, 2017), pp. 37–45, doi:10.1007/978-3-319-51085-9_4.

[73]M. M. Rhaman, M. A. Matin, M. A. Hakim and M. F. Islam, Dielectric, ferroelectric and ferromagnetic properties of samarium doped multiferroic bismuth ferrite, *Mater. Res. Express* **6**, 125080 (2019), doi:10.1088/2053-1591/ab57c2.

[74]V. Dillu, M. T. Kebede, S. Devi and S. Chauhan, Synthesis and characterization of samarium substituted bismuth ferrites nanoparticles, *Mater. Today, Proc.* **34**, 813 (2020), doi:10.1016/j.matpr.2020.05.348.

[75]Y. B. Yao, W. C. Liu and C. L. Mak, Pyroelectric properties and electrical conductivity in samarium doped $BiFeO_3$ ceramics, *J. Alloys Compd.* **527**, 157 (2012), doi:10.1016/j.jallcom.2012.02.182.

[76]R. S. N. Ain, S. A. Halim and M. Hashim, Effect of Sm-doping on magnetic and dielectric properties of $BiFeO_3$, *Adv. Mater. Res.* **501**, 329 (2012), doi:10.4028/www.scientific.net/amr.501.329.

[77]H. Singh and K. L. Yadav, Structural, dielectric, vibrational and magnetic properties of Sm doped $BiFeO_3$ multiferroic ceramics prepared by a rapid liquid phase sintering method, *Ceram. Int.* **41**, 9285 (2015), doi:10.1016/j.ceramint.2015.03.212.

[78]A. Awan, S. Riaz, A. Nairan, Y. B. Xu and S. Naseem, Tunable magnetic and dielectric properties of $BiFeO_3$ nanoparticles — Effect of lanthanum doping, *Proc. 2016 World Congr. Advances in Civil, Environmental and Materials Research* (2016), pp. 1–9.

[79]A. Kumari, K. Kumari, A. Vij, P. A. Alvi and S. Kumar, Electrical and structural properties of La doped $BiFeO_3$, *AIP Conf. Proc.* **2220**, 040032 (2020), doi:10.1063/5.0001563.

[80]D. S. García-Zaleta, A. M. Torres-Huerta, M. A. Domínguez-Crespo, J. A. Matutes-Aquino, A. M. González and M. E. Villafuerte-Castrejón, Solid solutions of La-doped $BiFeO_3$ obtained by the Pechini method with improvement in their properties, *Ceram. Int.* **40**, 9225 (2014), doi:10.1016/j.ceramint.2014.01.143.

[81]A. Chaudhuri and K. Mandal, Enhancement of ferromagnetic and dielectric properties of lanthanum doped bismuth ferrite nanostructures, *Mater. Res. Bull.* **47**, 1057 (2012), doi:10.1016/j.materresbull.2011.12.034.

[82]Y. Dua, Z. X. Cheng, M. Shahbazi, E. W. Collings, S. X. Dou and X. L. Wang, Enhancement of ferromagnetic and dielectric properties in lanthanum doped $BiFeO_3$ by hydrothermal synthesis, *J. Alloys Compd.* **490**, 637 (2010), doi:10.1016/j.jallcom.2009.10.124.

[83]S. R. Das, R. N. P. Choudhary, P. Bhattacharya and R. S. Katiyar, Structural and multiferroic properties of La-modified $BiFeO_3$ ceramics, *J. Appl. Phys.* **101**, 034104 (2007), doi:10.1063/1.2432869.

[84]N. Sheoran, A. Kumar, V. Kumar and A. Banerjee, Structural, optical, and multiferroic properties of yttrium (Y^{3+})-substituted $BiFeO_3$ nanostructures, *J. Supercond. Nov. Magn.* **33**, 2017 (2020), doi:10.1007/s10948-019-05411-2.

[85]H. Fki, M. Koubaa, L. Sicard, W. Cheikhrouhou-Koubaa, A. Cheikhrouhou and S. Ammar-Merah, Influence of Y doping on structural, vibrational, optical and magnetic properties of

BiFeO$_3$ ceramics prepared by mechanical activation, *Ceram. Int.* **43**, 4139 (2017), doi:10.1016/j.ceramint.2016.12.028.

[86]M. Arora and M. Kumar, Electron spin resonance probed enhanced magnetization and optical properties of Sm doped BiFeO$_3$ nanoparticles, *Mater. Lett.* **137**, 285 (2014), doi:10.1016/j.matlet.2014.08.140.

[87]M. B. Bellakki and V. Manivannan, Citrate-gel synthesis and characterization of yttrium-doped multiferroic BiFeO$_3$, *J. Sol-Gel Sci. Technol.* **53**, 184 (2009), doi:10.1007/s10971-009-2076-1.

[88]F.-C. Lü, K. Yin, K.-X. Fu, Y.-N. Wang, J. Ren and Q. Xie, Enhanced magnetic and dielectric properties of Y doped bismuth ferrite nanofiber, *Ceram. Int.* **43**, 16101 (2017), doi:10.1016/j.ceramint.2017.08.171.

[89]M. Zhong, N. Pavan Kumar, E. Sagar, Z. Jian, H. Yemin and P. Venugopal Reddy, Structural, magnetic and dielectric properties of Y doped BiFeO$_3$, *Mater. Chem. Phys.* **173**, 126 (2016), doi:10.1016/j.matchemphys.2016.01.047.

[90]R. K. Mishra, D. K. Pradhan, R. N. P. Choudhary and A. Banerjee, Effect of yttrium on improvement of dielectric properties and magnetic switching behavior in BiFeO$_3$, *J. Phys., Condens. Matter* **20**, 045218 (2008), doi:10.1088/0953-8984/20/04/045218.

[91]N. I. Ilić, J. D. Bobić, B. S. Stojadinović, A. S. Džunuzović, M. M. V. Petrović, Z. D. Dohčević-Mitrović and B. D. Stojanović, Improving of the electrical and magnetic properties of BiFeO$_3$ by doping with yttrium, *Mater. Res. Bull.* **77**, 60 (2016), doi:10.1016/j.materresbull.2016.01.018.

[92]B. K. Vashisth, J. S. Bangruwa, S. P. Gairola and V. Verma, Structural, dielectric, ferroelectric and magnetic properties of Gd doped BiFeO$_3$, *Integr. Ferroelectr.* **194**, 21 (2018), doi:10.1080/10584587.2018.1514869.

[93]S. Dabas, M. Kumar and O. P. Thakur, Investigation on structural, magnetic, dielectric and impedance spectroscopy properties of 'Gd' modified multiferroic-ferroelectric solid solutions, *Ceram. Int.* **46**, 17361 (2020), doi:10.1016/j.ceramint.2020.04.026.

[94]P. Suresh and S. Srinath, Crystal structure and enhanced dielectric, magnetic properties of Gd doped BiFeO$_3$ ceramics, *Mater. Focus* **2**, 201 (2013), doi:10.1166/mat.2013.1075.

[95]R. Guo, L. Fang, W. Dong, F. Zheng and M. Shen, Enhanced photocatalytic activity and ferromagnetism in Gd doped BiFeO$_3$ nanoparticles, *J. Phys. Chem. C* **114**, 21390 (2010), doi:10.1021/jp104660a.

[96]G. S. Lotey and N. K. Verma, Structural, magnetic, and electrical properties of Gd-doped BiFeO$_3$ nanoparticles with reduced particle size, *J. Nanopart. Res.* **14**, 742 (2012), doi:10.1007/s11051-012-0742-7.

[97]S. K. Pradhan and B. K. Roul, Effect of Gd doping on structural, electrical and magnetic properties of BiFeO$_3$ electroceramic, *J. Phys. Chem. Solids* **72**, 1180 (2011), doi:10.1016/j.jpcs.2011.07.017.

[98]J. Cyriac, J. C. John, N. Kalarikkal and S. Augustine, Tailoring the dielectric and magnetic properties of Eu-substituted BiFeO$_3$ nanoparticles, *Mater. Today, Proc.* **25**, 134 (2020), doi:10.1016/j.matpr.2019.12.186.

[99]S. R. Kulkarni, C. M. Kanamadi and B. K. Chougule, Magnetic and dielectric properties of Ni$_{0.8}$Co$_{0.1}$Cu$_{0.1}$Fe$_2$O$_4$+PZT composites, *J. Phys. Chem. Solids* **67**, 1607 (2006), doi:10.1016/j.jpcs.2006.01.117.

[100]K. Chakrabarti, K. Das, B. Sarkar and S. K. De, Magnetic and dielectric properties of Eu-doped BiFeO$_3$ nanoparticles by acetic acid-assisted sol-gel method, *J. Appl. Phys.* **110**, 103905 (2011), doi:10.1063/1.3662178.

[101]P. C. Sati, M. Kumar, S. Chhoker and M. Jewariya, Influence of Eu substitution on structural, magnetic, optical and dielectric properties of BiFeO$_3$ multiferroic ceramics, *Ceram. Int.* **41**, 2389 (2015), doi:10.1016/j.ceramint.2014.10.053.

[102]P. Uniyal and K. L. Yadav, Room temperature multiferroic properties of Eu doped BiFeO$_3$, *J. Appl. Phys.* **105**, 07D914 (2009), doi:10.1063/1.3072087.

[103]J. Liu, L. Fang, F. Zheng, S. Ju and M. Shen, Enhancement of magnetization in Eu doped BiFeO$_3$ nanoparticles, *Appl. Phys. Lett.* **95**, 022511 (2009), doi:10.1063/1.3183580.

[104]P. Vanga, R. V. Mangalaraja and M. Ashok, Effect of (Nd, Ni) co-doped on the multiferroic and photocatalytic properties of BiFeO$_3$, *Mater. Res. Bull.* **72**, 299 (2015), doi:10.1016/j.materresbull.2015.08.015.

[105]J. Zhao, X. Zhang, S. Liu, W. Zhang and Z. Liu, Effect of Ni substitution on the crystal structure and magnetic properties of BiFeO$_3$, *J. Alloys Compd.* **557**, 120 (2013), doi:10.1016/j.jallcom.2013.01.005.

[106]A. Kumar and K. L. Yadav, A systematic study on magnetic, dielectric and magnetocapacitance properties of Ni doped bismuth ferrite, *J. Phys. Chem. Solids* **72**, 1189 (2011), doi:10.1016/j.jpcs.2011.06.006.

[107]M. Nadeem, W. Khan, S. Khan, S. Husain and A. Ansar, Tailoring dielectric properties and multiferroic behavior of nanocrystalline BiFeO$_3$ via Ni doping, *J. Appl. Phys.* **124**, 164105 (2018), doi:10.1063/1.5050946.

[108]L. G. Betancourt-Cantera, A. M. Bolarín-Miró, C. A. Cortés-Escobedo, L. E. Hernández Cruz and F. Sánchez-De Jesús, Structural transitions and multiferroic properties of high Ni-doped BiFeO$_3$, *J. Magn. Magn. Mater.* **456**, 381 (2018), doi:10.1016/j.jmmm.2018.02.065.

[109]J. Khajonrit, N. Prasoetsopha, T. Sinprachim, P. Kidkhunthod, S. Pinitsoontorn and S. Maensiri, Structure, characterization, and magnetic/electrochemical properties of Ni-doped BiFeO$_3$ nanoparticles, *Adv. Nat. Sci., Nanosci. Nanotechnol.* **8**, 015010 (2017), doi:10.1088/2043-6254/aa597d.

[110]C.-H. Yang, D. Kan, I. Takeuchi, V. Nagarajan and J. Seidel, Doping BiFeO$_3$: Approaches and enhanced functionality, *Phys. Chem. Chem. Phys.* **14**, 15953 (2012), doi:10.1039/c2cp43082g.

[111]M. Daraktchiev, G. Catalan and J. F. Scott, Landau theory of domain wall magnetoelectricity, *Phys. Rev. B* **81**, 224118 (2010), doi:10.1103/physrevb.81.224118.

[112]V. Skumryev, V. Laukhin, I. Fina, X. Martí, F. Sánchez, M. Gospodinov and J. Fontcuberta, Magnetization reversal by electric-field decoupling of magnetic and ferroelectric domain walls in multiferroic-based heterostructures, *Phys. Rev. Lett.* **106**, 057206 (2011), doi:10.1103/physrevlett.106.057206.

[113]G. Catalan, J. Seidel, R. Ramesh and J. F. Scott, Domain wall nanoelectronics, *Rev. Mod. Phys.* **84**, 119 (2012), doi:10.1103/revmodphys.84.119.

[114]S. E. M. Ghahfarokhi, M. R. Larki and I. Kazeminezhad, The effect of Mn doped on the structural, magnetic, dielectric and optical properties of bismuth ferrite (BiFe$_{1-x}$Mn$_x$O$_3$) nanoparticles, *Vacuum* **173**, 109143 (2019), doi:10.1016/j.vacuum.2019.109143.

[115]B. Dhanalakshmi, B. Chandra Sekhar, K. V. Vivekananda, B. Srinivasa Rao, B. Parvatheeswara Rao and P. S. V. Subba Rao, Enhanced dielectric and magnetic properties in Mn-doped bismuth ferrite multiferroic nanoceramics, *Appl. Phys. A* **126**, 557 (2020), doi:10.1007/s00339-020-03745-6.

[116]R. R. Awasthi, K. Asokan and B. Das, Structural, dielectric and magnetic domains properties of Mn-doped BiFeO$_3$ materials, *Appl. Ceram. Technol.* **17**, 1410 (2019), doi:10.1111/ijac.13446.

[117]Y. J. Yoo, J. S. Hwang, Y. P. Lee, J. S. Park, J. Y. Rhee, J.-H. Kang, K. W. Lee, B. W. Lee and M. S. Seo, Origin of enhanced multiferroic

properties in Dy and Co co-doped $BiFeO_3$ ceramics, *J. Magn. Magn. Mater.* **374**, 669 (2015), doi:10.1016/j.jmmm.2014.09.034.

[118]S. Dong, J.-M. Liu, S.-W. Cheong and Z. Ren, Multiferroic materials and magnetoelectric physics: Symmetry, entanglement, excitation, and topology, *Adv. Phys.* **64**, 519 (2015), (doi:10.1080/00018732.2015.1114338.

[119]K. Wohlfeld, M. Daghofer and A. M. Oleś, Spin-orbital physics for *p* orbitals in alkali RO_2 hyperoxides — Generalization of the Goodenough-Kanamori rules, *Europhys. Lett.* **96**, 27001 (2011), doi:10.1209/0295-5075/96/27001.

[120]A. K. Sinha, B. Bhushan, Jagannath, R. K. Sharma, S. Sen, B. P. Mandal, S. S. Meena, P. Bhatt, C. L. Prajapat, A. Priyam, S. K. Mishra and S. C. Gadkari, Enhanced dielectric, magnetic and optical properties of Cr-doped $BiFeO_3$ multiferroic nanoparticles synthesized by sol-gel route, *Results Phys.* **13**, 102299 (2019), doi:10.1016/j.rinp.2019.102299.

[121]A. Kumar and K. L. Yadav, Magnetic, magnetocapacitance and dielectric properties of Cr doped bismuth ferrite nanoceramics, *Mater. Sci. Eng. B* **176**, 227 (2011), doi:10.1016/j.mseb.2010.11.012.

[122]I. M. Reaney, I. MacLaren, L. Wang, B. Schaffer, A. Craven, K. Kalantari, I. Sterianou, S. Miao, S. Karimi and D. C. Sinclair, Defect chemistry of Ti-doped antiferroelectric $Bi_{0.85}Nd_{0.15}FeO_3$, *Appl. Phys. Lett.* **100**, 182902 (2012), doi:10.1063/1.4705431.

[123]M. S. Bernardo, T. Jardiel, M. Peiteado, F. J. Mompean, M. Garcia-Hernandez, M. A. Garcia, M. Villegas and A. C. Caballero, Intrinsic compositional inhomogeneities in bulk Ti-doped $BiFeO_3$: Microstructure development and multiferroic properties, *Chem. Mater.* **25**, 1533 (2013), doi:10.1021/cm303743h.

[124]X. H. Zheng, Z. H. Ma, P. J. Chen, D. P. Tang and N. Ma, Decomposition behavior and dielectric properties of Ti-doped $BiFeO_3$ ceramics derived from molten salt method, *J. Mater. Sci., Mater. Electron.* **23**, 1533 (2012), doi:10.1007/s10854-012-0624-x.

[125]Y. Tian, F. Xue, Q. Fu, L. Zhou, C. Wang, H. Gou and M. Zhang, Structural and physical properties of Ti-doped $BiFeO_3$ nanoceramics, *Ceram. Int.* **44**, 4287 (2018), doi:10.1016/j.ceramint.2017.12.013.

[126]J. Seidel, W. Luo, S. J. Suresha, P. K. Nguyen, A. S. Lee, S. Y. Kim, C. H. Yang, J. Pennycook, S. T. Pantelides, J. F. Scott and R. Ramesh, Prominent electrochromism through vacancy-order melting in a complex oxide, *Nat. Commun.* **3**, 799 (2012), doi:10.1038/ncomms1799.

[127]N. Wang, X. Luo, L. Han, Z. Zhang, R. Zhang, H. Olin and Y. Yang, Structure, performance, and application of $BiFeO_3$ nanomaterials, *Nano-Micro Lett.* **12**, 81 (2020), doi:10.1007/s40820-020-00420-6.

[128]Z.-Z. Jiang, Z. Guan, N. Yang, P.-H. Xiang, R.-J. Qi, R. Huang, P.-X. Yang, N. Zhong and C.-G. Duan, Epitaxial growth of $BiFeO_3$ films on $SrRuO_3/SrTiO_3$, *Mater. Charact.* **131**, 217 (2017), doi:10.1016/j.matchar.2017.07.009.

[129]Y. Zhang, Y. Wang, J. Qi, Y. Tian, M. Sun, J. Zhang, T. Hu, M. Wei, Y. Liu and J. Yang, Enhanced magnetic properties of $BiFeO_3$ thin films by doping: Analysis of structure and morphology, *Nanomaterials* **8**, 711 (2018), doi:10.3390/nano8090711.

[130]V. R. Palkar and R. Pinto, $BiFeO_3$ thin films: Novel effects, *Pramana* **58**, 1003 (2002), doi:10.1007/s12043-002-0207-0.

[131]Y. P. Wang, L. Zhou, M. F. Zhang, X. Y. Chen, J. M. Liu and Z. G. Liu, Room-temperature saturated ferroelectric polarization in $BiFeO_3$ ceramics synthesized by rapid liquid phase sintering, *Appl. Phys. Lett.* **84**, 1731 (2004), doi:10.1063/1.1667612.

[132]Y.-H. Lee, J.-M. Wu, Y.-L. Chueh and L.-J. Chou, Low-temperature growth and interface characterization of $BiFeO_3$ thin films with reduced leakage current, *Appl. Phys. Lett.* **87**, 172901 (2005), doi:10.1063/1.2112181.

[133]G.-Z. Liu, C. Wang, C.-C. Wang, J. Qiu, M. He, J. Xing, K.-J. Jin, H.-B. Lu and G.-Z. Yang, Effects of interfacial polarization on the dielectric properties of $BiFeO_3$ thin film capacitors, *Appl. Phys. Lett.* **92**, 122903 (2008), doi:10.1063/1.2900989.

[134]S. M. H. Shah, A. Akbar, S. Riaz, S. Atiq and S. Naseem, Magnetic, structural, and dielectric properties of $Bi_{1-x}K_xFeO_3$ thin films using sol-gel, *IEEE Trans. Magn.* **50**, 2201004 (2014), doi:10.1109/tmag.2014.2310691.

[135]K. Sen, K. Singh, A. Gautam and M. Singh, Dispersion studies of La substitution on dielectric and ferroelectric properties of multiferroic $BiFeO_3$ ceramic, *Ceram. Int.* **38**, 243 (2012), doi:10.1016/j.ceramint.2011.06.059.

[136]L. Bai, M. Sun, W. Ma, J. Yang, J. Zhang and Y. Liu, Enhanced magnetic properties of co-doped $BiFeO_3$ thin films via structural progression, *Nanomaterials* **10**, 1798 (2020), doi:10.3390/nano10091798.

[137]F. Yan, M.-O. Lai, L. Lu and T.-J. Zhu, Enhanced multiferroic properties and valence effect of Ru-doped $BiFeO_3$ thin films, *J. Phys. Chem. C* **114**, 6994 (2010), doi:10.1021/jp1009127.

[138]F. Yan, T. J. Zhu, M. O. Lai and L. Lu, Enhanced multiferroic properties and domain structure of La-doped $BiFeO_3$ thin films, *Scr. Mater.* **63**, 780 (2010), doi:10.1016/j.scriptamat.2010.06.013.

[139]H. Schmid, Some symmetry aspects of ferroics and single phase multiferroics, *J. Phys., Condens. Matter* **20**, 434201 (2008), doi:10.1088/0953-8984/20/43/434201.

[140]H. Schmid, On a magnetoelectric classification of materials, *Int. J. Magn.* **4**, 337 (1973).

[141]J. Ryu, S. Priya, K. Uchino and H.-E. Kim, Magnetoelectric effect in composites of magnetostrictive and piezoelectric materials, *J. Electroceram.* **8**, 107 (2002), doi:10.1023/a:1020599728432.

[142]N. K. Mohanty, A. K. Behera, S. K. Satpathy, B. Behera and P. Nayak, Effect of dysprosium substitution on structural and dielectric properties of $BiFeO_3$-$PbTiO_3$ multiferroic composites, *J. Rare Earths* **33**, 639 (2015), doi:10.1016/s1002-0721(14)60465-8.

[143]I. Kaur and N. K. Verma, Magnetic and electric properties of BFO–NFO nanocomposites, *Mater. Sci. Semicond. Process.* **33**, 32 (2015), doi:10.1016/j.mssp.2015.01.032.

[144]A. Das, S. De, S. Bandyopadhyay, S. Chatterjee and D. Das, Magnetic, dielectric and magnetoelectric properties of $BiFeO_3$-$CoFe_2O_4$ nanocomposites, *J. Alloys Compd.* **697**, 353 (2017), doi:10.1016/j.jallcom.2016.12.128.

[145]K. P. Remya, R. Rajalakshmi and N. Ponpandian, Development of $BiFeO_3/MnFe_2O_4$ ferrite nanocomposites with enhanced magnetic and electrical properties, *Nanoscale Adv.* **2020**, 2968 (2020), doi:10.1039/d0na00255k.

[146]A. R. Khan, G. M. Mustafa, S. K. Abbas, S. Atiq, S. M. Ramay and S. Naseem, Flexible ferroelectric and magnetic orders in $BiFeO_3/MnFe_2O_4$ nanocomposites to steer wide range energy and data storage capability, *Results Phys.* **16**, 102956 (2020), doi:10.1016/j.rinp.2020.102956.

[147]H. Singh and K. L. Yadav, Synthesis and thermal, structural, dielectric, magnetic and magnetoelectric studies of $BiFeO_3$-$MgFe_2O_4$ nanocomposites, *J. Am. Ceram. Soc.* **98**, 574 (2014), doi:10.1111/jace.13316.

[148]P. Augustine, Y. Narayana and N. Kalarickal, Enhancement of room temperature magneto-electric coupling effect in perovskite-spinel $(1-x)BiFeO_3$–$xZnFe_2O_4$ nanocomposites, *Mater. Today, Proc.* **35**, 436 (2020), doi:10.1016/j.matpr.2020.02.948.

[149]A. Khalid, M. Saleem, S. Naseem, S. M. Ramay, H. M. Shaikh and S. Atiq, Magneto-electric coupling and multifunctionality in $BiFeO_3$–$CoFe_2O_4$ core-shell nano-composites, *Ceram. Int.* **46**, 12828 (2020), doi:10.1016/j.ceramint.2020.02.053.

[150]Y. Zhao, J. Li, Z. Yin, X. Zhang, J. Huang, L. Cao and H. Wang, Interface-mediated local conduction at tubular interfaces in

BiFeO$_3$–CoFe$_2$O$_4$ nanocomposites, *J. Alloys Compd.* **823**, 153699 (2020), doi:10.1016/j.jallcom.2020.153699.

[151]F. Akram, J. Kim, S. A. Khan, A. Zeb, H. G. Yeo, Y. S. Sung, T. K. Song, M.-H. Kim and S. Lee, Less temperature-dependent high dielectric and energy-storage properties of eco-friendly BiFeO$_3$–BaTiO$_3$-based ceramics, *J. Alloys Compd.* **818**, 152878 (2019), doi:10.1016/j.jallcom.2019.152878.

[152]H. Baqiah, Z. A. Talib, A. H. Shaar, M. M. Dihom, M. M. Awang Kechik, S. K. Chen, J. Y. C. Liew, Z. Zainal and L. M. Fudzi, Structural, optical, magnetic and photoelectrochemical properties of (BiFeO$_3$)$_{1-x}$(Fe$_3$O$_4$)$_x$ nanocomposites, *J. Sol-Gel Sci. Technol.* **91**, 624 (2019), doi:10.1007/s10971-019-05053-9.

[153]H. Pan, F. Li, Y. Liu, Q. Zhang, M. Wang, S. Lan, Y. Zheng, J. Ma, L. Gu, Y. Shen, P. Yu, S. Zhang, L.-Q. Chen, Y.-H. Lin and C.-W. Nan, Ultrahigh-energy density lead-free dielectric films via polymorphic nanodomain design, *Science* **365**, 578 (2019), doi:10.1126/science.aaw8109.

[154]C. Yang, J. Qian, P. Lv, H. Wu, X. Lin, K. Wang and Z. Cheng, Flexible lead-free BFO-based dielectric capacitor with large energy density, superior thermal stability, and reliable bending endurance, *J. Materiomics* **6**, 200 (2020), doi:10.1016/j.jmat.2020.01.010.

[155]Q. M. Zhang, H. Wang, N. Kim and L. E. Cross, Direct evaluation of domain-wall and intrinsic contributions to the dielectric and piezoelectric response and their temperature dependence on lead zirconate–titanate ceramics, *J. Appl. Phys.* **75**, 454 (1994), doi:10.1063/1.355874.

[156]C. A. Randall, N. Kim, J. P. Kucera, W. Cao and T. R. Shrout, Intrinsic and extrinsic size effects in fine-grained morphotropic-phase-boundary lead zirconate titanate ceramics, *J. Am. Ceram. Soc.* **81**, 677 (1998), doi:10.1111/j.1151-2916.1998.tb02389.x.